

# On the aspect ratio of 'Oumuamua : less elongated shape for irregular surface properties

Allona Vazan,<sup>1,2</sup>★ Re'em Sari,<sup>1</sup>

<sup>1</sup>Racah Institute of Physics, The Hebrew University, Jerusalem 91904, Israel

<sup>2</sup>Institute for Computational Science, Center for Theoretical Astrophysics & Cosmology University of Zurich, Switzerland.

## ABSTRACT

The large brightness variation in the observed lightcurve of 'Oumuamua is probably related to its shape, i.e., to the ratio between its longest axis and its shortest axis (aspect ratio). Several approaches found the aspect ratio of 'Oumuamua to be unusually elongated. Moreover, the spin axis orientation has to be almost perpendicular to the observer in order to obtain such an extreme lightcurve, a configuration which is unlikely. However, interstellar 'Oumuamua may have different surface properties than we know in our solar system. Therefore, in this work we widen the parameter space for surface properties beyond the asteroid-like models and study its effect on 'Oumuamua's lightcurve. We calculate reflection from a rotating ellipsoidal object for four models: Lambertian reflection, specular reflection, single scattering diffusive and backscatter. We then calculate the probability to obtain a lightcurve ratio larger than the observed, as a function of the object's aspect ratio, assuming an isotropic spin orientation distribution. We find the elongation of 'Oumuamua to be less extreme for the Lambertian and specular reflection models. Consequently, the probability to observe the lightcurve ratio of 'Oumuamua given its unknown spin axis orientation is larger for those models. We conclude that different surface reflection properties may suggest alternatives to the extreme shape of 'Oumuamua, relieving the need for complicated formation scenario, extreme albedo variation, or unnatural origin. Although the models suggested here are for ideal ellipsoidal shape and ideal reflection method, the results emphasize the importance of surface properties for the derived aspect ratio.

**Key words:** minor planets, asteroids: individual: 'Oumuamua

## 1 INTRODUCTION

'Oumuamua, likely an interstellar object and the first one to be observed, exhibited a variation of about factor ten in its brightness<sup>1</sup> (Meech et al. 2017; Jewitt et al. 2017; Bolin et al. 2018, etc.). This variation is linked mainly to the shape of 'Oumuamua, namely the ratio between its longest axis and its shortest axis (aspect ratio) ('Oumuamua ISSI Team 2019). The 'Oumuamua aspect ratio was derived in several approaches (e.g., Meech et al. 2017; Bolin et al. 2018; McNeill et al. 2018) and is found to be extreme and much higher than the aspect ratio of objects in the solar system. Naively, one can expect the lightcurve magnitude variation between the brightest and the dimmest states (lightcurve ratio) to be equal to the aspect ratio. Indeed, the first work by Meech et al. (2017) fits the observed lightcurve ratio of 10 with a body of aspect ratio of

10, where the effect of the angle between the Sun and the observer (phase angle) is neglected.

Previous estimates of the aspect ratio of 'Oumuamua are based on reflection from asteroid-like objects: Meech et al. (2017) aspect ratio of 10 is based on Detal et al. (1994), where the projection of the object is calculated assuming zero phase angle. Bolin et al. (2018) accounted for the actual phase angle and derived aspect ratio ranging from 4:1 to 10:1, based on the formulation of Barucci & Fulchignoni (1982) for different models of asteroids. Mashchenko (2019) finds aspect ratio of 8 to be most probable by using Lommel-Seeliger reflection (Lumme & Bowell 1981). A somewhat lower aspect ratio of  $6 \pm 1$  is found by McNeill et al. (2018) using the lightcurve inversion model of Durech et al. (2010). This elongation is less than some other estimates, but still remarkable.

Nevertheless, elongation is expected to be greater than that. The above works assume the most favorable condition where the spin axis is perpendicular to the Sun - 'Oumuamua - Earth (hereafter SOE) plane. If the spin axis is not perpendicular to the SOE plane the observed lightcurve ratio becomes smaller, i.e., the aspect ratio of the body has to be larger. Thus, the resulting aspect ratios mentioned above are only lower limit for the real body's aspect ratio. The probability to observe an interstellar elongated object when its spin

★ E-mail: allona.vazan@mail.huji.ac.il

<sup>1</sup> Brightness variation is found to range between 4.5-12 in different observations. While Meech et al. (2017) observed a lightcurve ratio ( $L_{\max}/L_{\min}$ ) of more than 10 (2.5 mag), the lightcurve ratio is between 6 and 9 ( $2 \pm 0.2$  mag) in Jewitt et al. (2017), and as low as 4.5-8.2 (1.2-2.1 mag) in Bolin et al. (2018). Here we take brightness ratio of 10 as the standard.

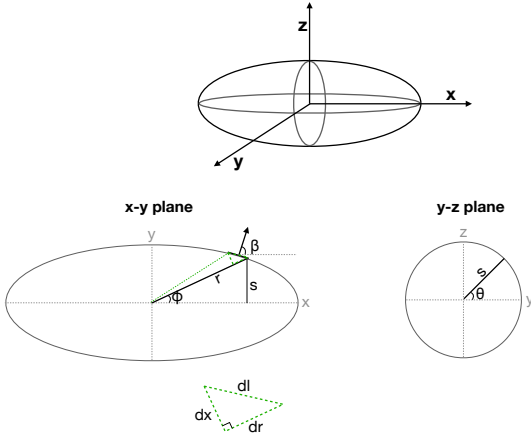


**Figure 1.** Geometry of the ellipsoid in our models. The dashed green rectangle is a zoom-in of the similar rectangle in the ellipse.

is exactly perpendicular to Earth is low. Since the orientation of 'Oumuamua spin axis is unknown, there is higher probability that the 'Oumuamua aspect ratio is larger than these lower limits, i.e. even more irregular (e.g., Mashchenko 2019; Siraj & Loeb 2019).

It is well known that surface properties affect the light reflectance (Chandrasekhar 1960; Lester et al. 1979). The surface materials of some of the airless bodies in the solar system exhibit the opposition effect, which is a strong tendency to reflect light backward, to the source. Other bodies are well described by the Lommel-Seeliger law, a single scattering diffusive reflection (e.g., Muinonen & Lumme 2015). However, irregular surface properties, different than the typical properties of solar system objects, might be more probable than the irregular shape that is derived for 'Oumuamua. Therefore, in this work we widen the parameter space for surface properties beyond the asteroid-like models.

In section 2 we calculate reflection from a rotating ellipsoid from basic principles. We consider two extreme reflection cases: the perfect diffusive (Lambertian), and the mirror (specular). We calculate also single scattering diffusive (Lommel-Seeliger) reflection, and backscatter (projected area) reflection, which are relevant to objects in our solar system. In section 3 we derive the minimal aspect ratio of 'Oumuamua for each method (obtained if the spin axis is perpendicular to the SOE), as well as the probability to get the observed lightcurve ratio (or larger) as function of the aspect ratio. We discuss the conditions for the suggested models and draw our conclusions in section 4.

## 2 METHODS

We assume that 'Oumuamua physical shape is a spheroid with axis ratio  $a:b$ ,  $a > b$ , and that it has a uniform albedo. The object reflectance in each rotation angle is calculated ab-initio by integration over reflection from infinitesimal area elements on the surface of the ellipsoid. Spin axis orientation, and phase angle ( $\Theta$ ) are naturally included.

### 2.1 Model geometry

First we calculate the surface area elements of the ellipsoid. The coordinates are fixed in the body's frame, as is shown in Fig. 1. The

long axis of the ellipsoid is the x-axis, while the spin axis, parallel to the short axis of the ellipsoid is the z axis. For simplicity, the elements are built by multiplying intervals on ellipses in the x-y plane by intervals on circles in the y-z plane (see Fig. 1). The 2D ellipse (x-y) radius is described in respect to the azimuthal angle  $\phi$  and the axes (a,b):

$$r(\phi) = \frac{a \cdot b}{\sqrt{a^2 \sin^2 \phi + b^2 \cos^2 \phi}} \quad (1)$$

In order to calculate the length interval ( $dl$ ) in the x-y plane, we build a Pythagoras rectangle for each surface interval (see green dashed rectangle in Fig. 1). We use the change in ellipse radius with angle:

$$dr(\phi) = \frac{a \cdot b}{2} \cdot \frac{\sin(2\phi) \cdot (b^2 - a^2)}{(a^2 \sin^2 \phi + b^2 \cos^2 \phi)^{3/2}} \cdot d\phi \quad (2)$$

and the radius interval of a circular object:  $dx(\phi) = r(\phi) \cdot d\phi$ . The surface interval in x-y plane is then

$$dl(\phi) = \sqrt{dr(\phi)^2 + dx(\phi)^2} \quad (3)$$

The surface normal angle  $\beta$  for each surface interval  $dl$  is derived from  $\phi$ :

$$\beta(\phi) = \phi + \arctan \frac{dr(\phi)}{dx(\phi)} \quad (4)$$

In the y-z plane the surface intervals are of circular geometry (since  $b=c$ ), in respect to the polar angle ( $\theta$ ). The radius of each circle is determined by its location on the x-y plane ellipse:  $s(\phi) = r(\phi) \cdot \sin \phi$ . Thus, surface interval in the y-z plane is

$$ds(\theta, \phi) = s(\phi) \cdot d\theta = r(\phi) \cdot \sin \phi \cdot d\theta \quad (5)$$

The size of each surface element is calculated from the above geometry, and results in

$$dA(\theta, \phi) = dl(\phi) \cdot ds(\theta, \phi) \quad (6)$$

The normal of each surface area element is then determined by  $\beta$  and  $\theta$ , forming a matrix of surface normals of the ellipsoid:

$$\hat{A}_x = \cos \beta; \quad \hat{A}_y = \sin \beta \cos \theta; \quad \hat{A}_z = \sin \beta \sin \theta \quad (7)$$

The Sun (projector) and the Earth (observer) are located in:

$$\hat{N}_\odot = [\cos \theta_\odot \cdot \cos \phi_\odot; \cos \theta_\odot \cdot \sin \phi_\odot; \sin \theta_\odot] \quad (8)$$

$$\hat{N}_\oplus = [\cos \theta_\oplus \cdot \cos \phi_\oplus; \cos \theta_\oplus \cdot \sin \phi_\oplus; \sin \theta_\oplus]$$

These angles are related to the phase angle  $\Theta$  by  $\cos \Theta = \hat{N}_\odot \cdot \hat{N}_\oplus$ . The effect of the rotation axis orientation on the lightcurve is obtained by varying  $\phi_\odot, \phi_\oplus$ . For 'Oumuamua, where the phase angle is known, we consider only SOE configurations that are consistent with this known value.

The observed brightness ratio depends also on the spin axis orientation in respect to the SOE plane. Since the spin axis orientation of 'Oumuamua is unknown, we vary this parameter. First, we assume that the spin axis orientation is perpendicular to the SOE (hereafter perpendicular spin). Perpendicular spin results in the largest lightcurve ratio for given SOE and object, and the results in Sec. 3.1 are under this assumption. We relax this assumption in Sec. 3.2, when we allow for various spin axis orientations and calculate the probability to observe 'Oumuamua lightcurve for different aspect ratios.

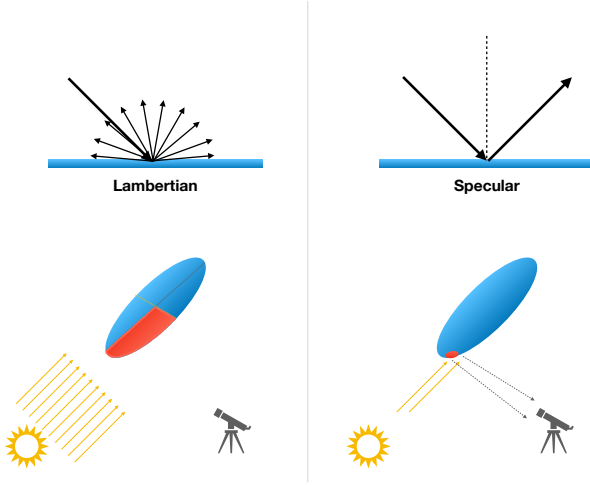


**Figure 2.** An illustration of Lambertian (left) and specular (right) reflection. Up: reflection from a plane unit surface area. Bottom: overall reflection from an ellipsoid. The surface area on each ellipsoid that contributes the observed brightness appears in red.

## 2.2 Model assumptions

(1) We assume the geometry of the 'Oumuamua to be ellipsoid with  $a > b = c$ , i.e., an elongated shape. The elongated (cigar-like) shape is more likely than a flat (pancake-like) shape, both because it is more energetically stable and because it has a larger range of possible orientations (Belton et al. 2018; Katz 2018; 'Oumuamua ISSI Team 2019). We therefore ignore the pancake-like shape, although it was found to be more probable by Mashchenko (2019). The assumption of  $b = c$  is consistent with calculation by Belton et al. (2018), that found  $b = 1.03c$  for a cigar shape.

(2) We take the SOE location and distances to be constant during rotation period. To make this assumption we compare the 'Oumuamua rotational period time ( $\sim 8$  hr) with the location change in this time. With an average velocity of  $26$  km/s the change in location within a rotation period can be as much as  $0.005$  AU. This distance is small in comparison to 'Oumuamua closet point to Earth ( $0.16$  AU).

(3) We assume a constant phase angle, because the SOE location is nearly constant during one rotation period. During the overall observation period of 'Oumuamua, the phase angle changed between  $19^\circ - 27^\circ$ , and up to  $24^\circ$  for the mag  $\geq 2.2$  observation period (Jewitt et al. 2017; Bolin et al. 2018; McNeill et al. 2018; Belton et al. 2018). Therefore we calculate here for  $\Theta = 2\pi/15 = 24^\circ$ , but also consider cases of  $\Theta = \pi/9 = 20^\circ$ , to show the effect of phase angle on the results.

(4) We assume a uniform albedo for simplicity.

(5) We assume rotation only around the z-axis (see Fig. 1) from minimum energy consideration.

(6) We ignore tumbling for simplicity of the model. 'Oumuamua photometry data suggests that it is tumbling (Fraser et al. 2018; Belton et al. 2018), as the lightcurve and rotation time change between different periods. These variations are of order 10%.

(7) We ignore the difference in lightcurve ratio between October and November measurements (Belton et al. 2018).

## 2.3 Surface reflection

**Lambertian surface:** If 'Oumuamua has a matte (perfect diffusive, Lambertian) surface, the apparent brightness from a surface element is the same for all observe angles of view (see Fig. 2 upper left). For a finite surface element the reflectance from Lambertian surface is determined by the incident flux angle ( $\cos \psi_i$ ), but also by the scattered flux angle ( $\cos \psi_s$ ) which affects the angular size of this element (e.g., Durech et al. 2010). The flux from each infinitesimal surface element is then

$$dF \propto dA \cdot \cos \psi_i \cdot \cos \psi_s \quad (9)$$

where

$$\cos \psi_i = \hat{dA} \cdot \hat{N}_\odot; \quad \cos \psi_s = \hat{dA} \cdot \hat{N}_\oplus \quad (10)$$

The overall flux is obtained by integration of  $dF$  over all ellipsoidal surface elements that are both illuminated ( $\cos \psi_i > 0$ ) and observable ( $\cos \psi_s > 0$ ), as marked in red in the bottom left of Fig. 2.

**Specular reflection:** Here we take 'Oumuamua to be a perfectly polished ellipsoid, acting as a mirror (specular reflection). For a given ellipsoid position and orientation, reflection is received from a single point on the surface, where the surface normal ( $\hat{dA}$ ) is in the same direction as the bisector of the SOE angle, i.e. parallel to  $\hat{N}_\oplus + \hat{N}_\odot$ , as is shown in the right panels of Fig. 2. The reflected intensity is inversely proportional to the curvature at this point as more curved surface scatters in a wider solid angle. Thus, for an axis symmetric body, the reflected flux is proportional to:

$$F \propto \frac{dl(\phi_r)}{d\beta} \cdot \frac{r(\phi_r) \cdot \sin \phi_r}{\sin \beta} \quad (11)$$

where  $\phi_r$  is the coordinate of the point of reflection - the point where the surface normal is parallel to the SOE bisector. For an ellipsoid, Eq. 11 can be calculated analytically:

$$F(\phi_r) \propto \frac{a^2 b^2 \left( a^2 \sin^2 \phi_r + \frac{b^4}{a^2} \cos^2 \phi_r \right)^2}{\left( a^2 \sin^2 \phi_r + b^2 \cos^2 \phi_r \right) \left( a^2 b^2 \sin^2 \phi_r + b^4 \cos^2 \phi_r \right)} \quad (12)$$

Note, that due to the axis symmetry of the body, the flux depends only on  $\phi$  and not on  $\theta$ . When we set the angle in Eq. 12 to the extreme values of  $\phi = 0$  and  $\phi = \pi/2$ , which are obtained for perpendicular spin, we find that the lightcurve ratio for ellipsoid with specular surface is as high as  $(a/b)^4$ . Such a ratio is extreme - ellipsoid with  $a/b = 2$  produces a lightcurve ratio of 16! This is a result of the extreme assumptions of a perfect mirror surface and a perfect ellipsoidal shape. Any perturbation on the shape or in the surface smoothness will lower this ratio, i.e., the perfect specular reflection provides the most extreme change of lightcurve ratio with aspect ratio.

**Backscatter:** The simplest case of reflection is the projected area law (e.g., Connelly & Ostro 1984). When the Sun and the observer are in the same object-centric direction (zero phase angle) the area of projection of the ellipsoid toward Earth direction is the cross-section of the ellipsoid geometry. In this case the lightcurve max/min ratio is proportional to the aspect ratio of the ellipsoid. The projected area law is used to model backscatter reflection, where radiation is reflected back toward the Sun. In a perfect backscatter process all radiation is reflected back and the object is not seen if the phase angle is not zero. In a non-perfect backscatter reflection most of the light is reflected back, but some light is reflected in

other directions, with the intensity decreases as the angle from the Sun direction gets larger (actually the phase angle). The key point is that the intensity variation depends only on the phase angle, and is independent of the object orientation. Therefore, since the phase angle is approximately constant<sup>2</sup> the observed lightcurve ratio is proportional to the projected area ratio. The flux from a surface element is then:

$$dF \propto dA \cdot \cos \psi_i \quad (13)$$

The total flux is the sum over all surface elements with  $\cos \psi_i > 0$  and  $\cos \psi_s > 0$ .

**Lommel-Seeliger model:** Lightcurve inversion models are usually derived under the assumption that the light-scattering behaviour of asteroids can be described as a combination of single-scatter diffusive (Lommel-Seeliger) and Lambertian models (e.g., Durech et al. 2010). Moreover, the Lommel-Seeliger model is a simple model that fits well the more detailed Hapke model for asteroids (Hapke 2002, 2012; Huang et al. 2017). Therefore, we calculate also reflectance from Lommel-Seeliger surface. Here, the contribution of each surface area element is determined by the incident flux angle ( $\psi_i$ ) and the scattered flux angle ( $\psi_s$ ) via (e.g., Fairbairn 2005; Durech et al. 2010):

$$dF \propto dA \cdot \frac{\cos \psi_i \cdot \cos \psi_s}{\cos \psi_i + \cos \psi_s} \quad (14)$$

Also here, we sum over all surface elements with  $\cos \psi_i > 0$  and  $\cos \psi_s > 0$  to get the total flux.

For each of the surface reflection models we repeat the calculation for all rotation angles along one period ( $2\pi$ ), for a given spin axis orientation. By that we actually assume that the spin axis is always around the short axis (z direction in Fig. 1). Then, we take the ratio of the maximum value to the minimum value of the intensity vector to be the lightcurve ratio.

## 2.4 Lightcurve ratio probability

For a given body shape and reflectance properties, the observed lightcurve ratio depends on the spin axis orientation. Since 'Oumuamua spin axis orientation is unknown, we calculate the lightcurve ratio for all possible rotation axis orientations. The spin axis orientation is defined by its azimuthal ( $\phi_s$ ) and polar ( $\theta_s$ ) angles. For each model we calculate the lightcurve ratio with a given aspect ratio for  $10^6$  cases of spin axis orientations distributed isotropically. Using these  $10^6$  results for the lightcurve ratio, we calculate the probability that the lightcurve ratio is above the observed value.

The probability that we discuss here is the probability to observe a lightcurve ratio above the observed value, for a given surface properties given a random orientation of the spin direction. This probability should not be interpreted as the probability that the object has such surface properties. The backscatter and Lommel-Seeliger surface properties are more in line with the scattering properties of objects in our solar system than the Lambertian or specular reflection surfaces.

<sup>2</sup> Phase angle variation is small during 'Oumuamua's rotation period, see model assumptions.

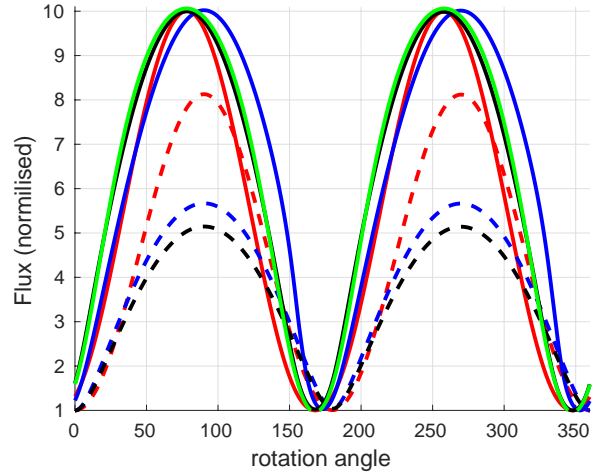


**Figure 3.** Calculated lightcurves for spinning ellipsoids with different surface reflection properties: Lambertian (blue), specular (green), backscatter (red), and Lommel-Seeliger (black). Solid curves are for phase angle of  $\Theta = 24^\circ$ , where the aspect ratio of each ellipsoid (3.5, 1.8, 5.5 and 5 respectively) were chosen to achieve the observed lightcurve ratio of 10. Dashed curves are for the same aspect ratios with  $\Theta = 0^\circ$ . Rotation spin axis is perpendicular to the SOE plane.

## 3 RESULTS

In section 3.1 we calculate the minimal aspect ratio needed to obtain a certain lightcurve ratio, assuming perpendicular spin (i.e., the largest lightcurve ratio for a given aspect ratio). In section 3.2 we calculate the probability to observe a lightcurve ratio equal or above the observed ratio, as a function of the aspect ratio of the body, assuming an isotropic spin distribution.

### 3.1 Minimal aspect ratio

For each of the models we calculate the reflection vs. rotation angle within one rotation period, and vary the aspect ratio in order to achieve a lightcurve ratio of 10. For zero phase angle ( $\Theta = 0$ ), the backscatter reflection as well as the reflection by Lommel-Seeliger model require aspect ratio of 10, as expected. When a phase angle of  $\Theta = 24^\circ$  is applied the lightcurve ratio of 10 is obtained by aspect ratio of  $\sim 5.5$  for backscatter reflection and  $\sim 5$  for Lommel-Seeliger surface reflection.

However, if the surface is Lambertian the minimal aspect ratio is as small as  $\sim 3.5$  with  $\Theta = 24^\circ$ , and of  $\sim 4$  with zero phase angle<sup>3</sup>. Specular surface requires aspect ratio of only  $\sim 1.8$  to provide 10 lightcurve ratio, and is independent of phase angle. These values, although calculated for extreme surface properties, are much lower than what was found in previous works. Thus, if 'Oumuamua's surface reflection properties significantly differ from those of asteroids, its shape might be much less elongated.

In Fig. 3 we show that for a finite phase angle ( $\Theta = 24^\circ$ ) the lightcurve ratio is larger than for zero phase angle. The calculated lightcurves for all reflection models are shown in the figure. The solid curves are for the above aspect ratios to get brightness ratio

<sup>3</sup> Changing the phase angle to  $\Theta = 20^\circ$  results in aspect ratio of 6 for backscatter model, 3.6 for Lambertian surface, and 5.4 for Lommel-Seeliger surface.

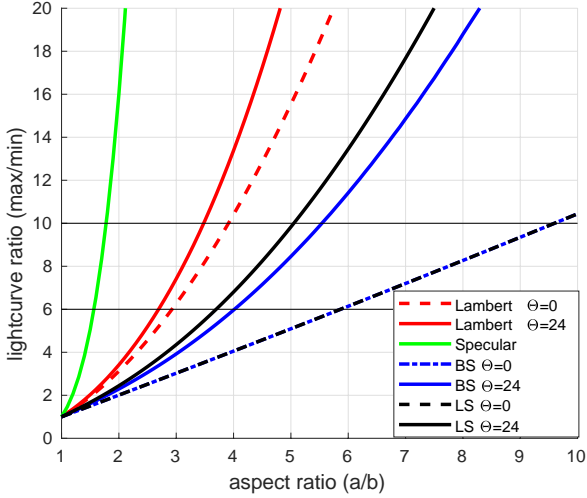


**Figure 4.** Lightcurve ratio as a function of the aspect ratio of ellipsoids ( $b=c$ ), for different surface reflection conditions: Lambertian (red), specular (green), backscatter (blue), and Lommel-Seeliger (black). Dashed curves are for phase angle  $\Theta = 0^\circ$  and solid for  $\Theta = 24^\circ$ . The green curve for specular reflection is independent of the phase angle. Rotation axis is perpendicular to the SOE plane for all cases.

of 10 with a phase angle of  $\Theta = 24^\circ$ . The dashed lines are for the same objects, but with  $\Theta = 0^\circ$ .

The effect of phase angle is not similar for different reflection methods. The greatest effect of the phase angle is for backscatter reflection and for the Lommel-Seeliger reflection. For Lambertian surface the phase angle effect is smaller. Although the phase angle changes the overlap between the incident flux area and the seen area (as is shown in Fig. 2), the isotropic flux by the Lambertian surface diminishes this effect. The specular reflection amplitude is not affected by the phase angle, since for any phase angle there is a given surface element in the SOE plane that reflects the flux (as is shown in Fig. 2). Therefore, the lightcurve is shifted, but the max/min ratio remains the same.

In Fig. 4 we show how the lightcurve ratio (max/min) changes as a function of the aspect ratio ( $a/b$ ) of the object. We consider cases with phase angle contribution ( $\Theta = 24^\circ$ ) and without ( $\Theta = 0^\circ$ ). The observed lightcurve ratio of 10 (Meech et al. 2017) and 6 (Jewitt et al. 2017) are marked (horizontal lines). The intersection of the observed lightcurve with a model curve marks the minimum aspect ratio for this model. The dependence of the lightcurve ratio on the aspect ratio, i.e., the slope of the curve, differs between the surface models. The Lambertian surface and the specular surface have steeper slopes and thus smaller aspect ratio to explain the 'Oumuamua observations, in comparison to the other models. As expected, the effect of phase angle, which was shown in Fig. 3, is greater as the aspect ratio increases for the same surface conditions.

Our calculation were done for a lightcurve ratio of 10. However, 'Oumuamua brightness variation ranges between 4.5-12 in different observations. For a lightcurve ratio lower than 10 the aspect ratios get smaller, as is shown in Fig. 4. For example, if we consider a lightcurve ratio of 6, the elongation of 'Oumuamua with Lambertian surface is only 2.7, while the Lommel-Seeliger and backscatter reflection models results in 3.7 and 4 respectively. For the perfect specular reflection surface the aspect ratio is as small as 1.55.

### 3.2 Probability to observe 'Oumuamua's lightcurve ratio

The minimal aspect ratio calculated in the previous section would result in the observed lightcurve of 'Oumuamua only if the spin axis orientation is exactly perpendicular. As this is unlikely, 'Oumuamua must have a higher aspect ratio to be observed with such a lightcurve ratio. Here, we calculate the probability to observe 'Oumuamua lightcurve ratio, as a function of the object's aspect ratio assuming an isotropic spin orientation. In Fig. 5 we show the lightcurve ratio (color coded) for ellipsoids with aspect ratio of  $a/b = 6$ . The lightcurve ratio is presented as a function of the angle between the spin axis and the Sun and the Earth orientation ( $\theta_\oplus, \theta_\odot$  in Eq. 8). We assume rotation only around the short ( $c$ ) axis, from minimal energy consideration, and ignore tumbling (see model assumptions). The white areas in the panels of Fig. 5 are excluded angles as they could not be realised with the phase angle of  $\Theta = 24^\circ$ .

To calculate the probability we give each point an appropriate weight according to an isotropic distribution of the spin axis orientation, and a fixed phase angle. The probability to observe a lightcurve ratio higher than 10 (dark red in Fig. 5) when the object has aspect ratio of 6 is about 3% (backscatter), 9% (Lommel-Seeliger), 30% (Lambertian) and 97% (specular). For specular reflection (right) the lightcurve ratio strongly depends on the aspect ratio (up to  $(a/b)^4$  for perpendicular spin), and therefore the probability is high even for moderate aspect ratio - aspect ratio of 2 has probability of 53% to observe a lightcurve ratio higher than 10.

For specular reflection model, we are able to obtain this probability analytically. A given lightcurve ratio  $n$  can be observed by an angle  $\phi_m$ , satisfying

$$\frac{F(\pi/2)}{F(\phi_m)} = n, \quad (15)$$

where  $F$  is given by Eq. 12. The probability to observe light curve ratio larger than  $n$  is now given by  $\cos \phi_m$ . We find the probability to observe a lightcurve ratio of  $n$  or larger from an ellipsoid with specular surface reflection as a function of its aspect ratio ( $a/b$ ) to be:

$$P = \frac{\sqrt{\left(\frac{a}{b}\right)^2 - \sqrt{n}}}{\sqrt{\left(\frac{a}{b}\right)^2 - 1}} \quad (16)$$

In Fig. 6 we show probability to observe a light curve ratio larger than 10 (left) and 6 (right) as a function of the ellipsoid aspect ratio. All calculations are for a phase angle  $\Theta = 24^\circ$ . As is shown in the figure, this probability increases with the aspect ratio up to a maximum probability. The increase depends on the model reflection method, namely how lightcurve ratio changes with aspect ratio (the slope in Fig. 4). For that reason the probability to observe a given lightcurve ratio is higher for Lambertian surface object and much higher for the specular surface, because of their stronger dependency of lightcurve ratio on aspect ratio. However, the probabilities calculated here are not the likelihood to form such a surface, which might be lower for the Lambertian and specular models, based on the knowledge from our solar system.

## 4 DISCUSSION AND CONCLUSIONS

Since 'Oumuamua is believed to be an interstellar object (Higuchi & Kokubo 2019) it might have different composition, age and history, than a solar system asteroid. As a result, its surface may differ from

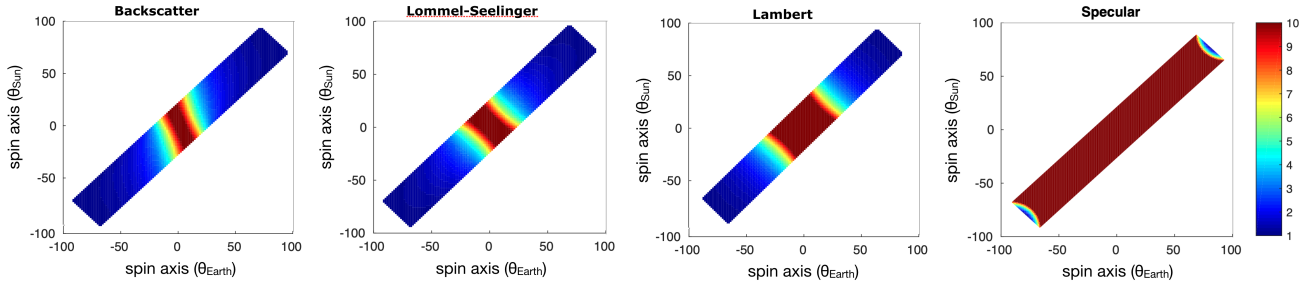


**Figure 5.** Color coded contours of the Lightcurve ratio from rotating ellipsoids of aspect ratio 6 as function of the spin axis angles for the four surface reflection properties: backscatter (left), Lommel-Seeliger surface (2nd), Lambertian surface (3rd), and specular reflection (right). In all case a fixed phase angle of  $\Theta = 24^\circ$  is assumed. The probability to observe a lightcurve ratio higher than 10 when the object has aspect ratio of 6 is about 3% (backscatter), 9% (Lommel-Seeliger), 30% (Lambertian) and 97% (specular).

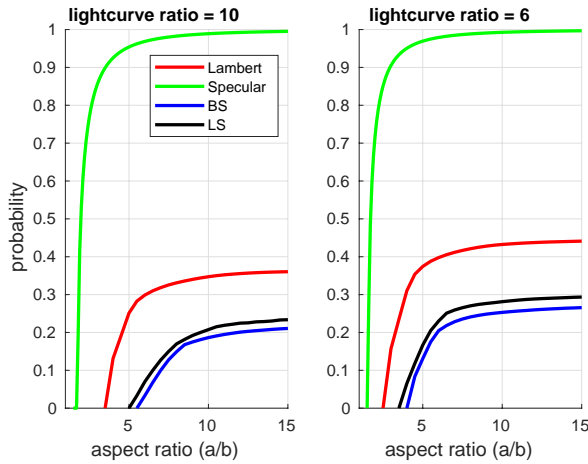


**Figure 6.** The probability to observe a lightcurve ratio of minimum 10 (left) and 6 (right) as a function of the object aspect ratio, for different surface reflection conditions: Lambertian (red), specular (green), backscatter (blue), and Lommel-Seeliger (black). For all cases phase angle is  $\Theta = 24^\circ$ .

what we know. We show that the elongation of 'Oumuamua can be much lower than predicted in previous models, by varying the surface reflection properties beyond the asteroid-like models. The less elongated shape relieves the need for extreme albedo changes (Mashchenko 2019), or unnatural origin (Bialy & Loeb 2018).

The question hence is what conditions can result in such surface properties. The surface properties of the rocky objects in the solar system are determined by the mineral crystallization as an outcome of the solar system composition and its formation. Different composition (as may be in other solar system), thermal history (heating), and dynamical history (friction, impacts) may result in different surface properties. For example, processes that 'Oumuamua may went through could melted it, like repeated flybys close to its star (Raymond et al. 2018), or heating by a red giant star (Katz 2018). If 'Oumuamua is in addition a metal rich object, its current surface (after melting) may be glossy. However, there is a very small chance that a natural object has a perfect mirror surface. Space weathering during 'Oumuamua interstellar travel could also changed its surface properties. In addition, the estimated age of 'Oumuamua is less than 1 Gyr (Almeida-Fernandes & Rocha-Pinto 2018), much less than small objects in the solar system.

The photometry data of 'Oumuamua (reflectivity vs. wave-

length) was compared to solar system spectral types. The spectral type of 'Oumuamua is found to be close to D-type asteroids, Trojan asteroids, inner solar system populations, and small trans-Neptunian objects (Meech et al. 2017; Jewitt et al. 2017; Bannister et al. 2017). Still, error bars on the measurements are too large to determine whether it is similar to the solar-system objects (e.g., Fig. 5 in Jewitt et al. 2017). Moreover, spectral type does not give a unique characterisation of the surface properties.

From probability perspective, the extreme lightcurve that was observed for 'Oumuamua indicates a spin axis orientation that is near perpendicular to the SOE plane. Small angles between the spin axis and the SOE plane cannot produce such a high lightcurve ratio, regardless of the object aspect ratio. Thus, the probability to get the observed lightcurve ratio is low, even for elongated bodies. As is shown in Fig. 6, this maximum probability varies for the different surface models. As an outcome, the Lambertian and specular reflection models are found to allow for 'Oumuamua observed lightcurve ratio with higher probability than the backscatter and the Lommel-Seeliger models. Yet, if our solar system is indicative, the formation of Lambertian or specular surface is less likely.

To summarise, as a first observed interstellar object, 'Oumuamua introduced new challenges to small bodies theories. Some of the challenges are related to the irregular elongated shape that is derived from its lightcurve ratio. We show that if the surface reflection properties of 'Oumuamua significantly differ from those of asteroids, its shape might be much less elongated. Those surface properties are also found to have higher probability to produce the observed lightcurve ratio of 'Oumuamua, given that its spin axis orientation is unknown. Although the models suggested here are for ideal ellipsoidal shape and ideal reflection method, the results emphasis the importance of surface properties for the derived aspect ratio.

In the coming years the interstellar object database is expected to grow (e.g., Trilling et al. 2018). Recently, a second interstellar object was detected, 2I/Borisov. Unlike 'Oumuamua, 2I/Borisov is a comet-like object, with similar properties to solar system comets (e.g., Guzik et al. 2019; Jewitt & Luu 2019). Detection of more interstellar objects will help us understand their nature, and how different their surface properties are from what we know.

## ACKNOWLEDGEMENTS

We would like to thank the referee for the useful comments. We also like to thank Josef Durech, Karri Muinonen, and David Polishook

for interesting comments and discussions. This research is partially supported by an Icore grant and an ISF grant.

## REFERENCES

- Almeida-Fernandes F., Rocha-Pinto H. J., 2018, *MNRAS*, **480**, 4903  
 Bannister M. T., et al., 2017, *ApJ*, **851**, L38  
 Barucci M. A., Fulchignoni M., 1982, *Moon and Planets*, **27**, 47  
 Belton M. J. S., et al., 2018, *ApJ*, **856**, L21  
 Bialy S., Loeb A., 2018, *ApJ*, **868**, L1  
 Bolin B. T., et al., 2018, *ApJ*, **852**, L2  
 Chandrasekhar S., 1960, *Radiative transfer*  
 Connelly R., Ostro S. J., 1984, *Geometriae Dedicata (ISSN 0046-5755)*, **17**, 87  
 Detal A., Hainaut O., Pospieszalska-Surdej A., Schils P., Schober H. J., Surdej J., 1994, *A&A*, **281**, 269  
 Durech J., Sidorin V., Kaasalainen M., 2010, *A&A*, **513**, A46  
 Fairbairn M. B., 2005, *J. R. Astron. Soc. Canada*, **99**, 92  
 Fraser W. C., Pravec P., Fitzsimmons A., Lacerda P., Bannister M. T., Snodgrass C., Smolić I., 2018, *Nature Astronomy*, **2**, 383  
 Guzik P., Drahus M., Rusek K., Waniak W., Cannizzaro G., Pastor-Marazuela I., 2019, *Nature Astronomy*, p. 467  
 Hapke B., 2002, *Icarus*, **157**, 523  
 Hapke B., 2012, *Icarus*, **221**, 1079  
 Higuchi A., Kokubo E., 2019, arXiv e-prints, p. arXiv:1911.04524  
 Huang X.-J., Lu X.-P., Li J.-Y., Mei B., Hsia C.-H., Zhao H.-B., 2017, *Research in Astronomy and Astrophysics*, **17**, 106  
 Jewitt D., Luu J., 2019, arXiv e-prints, p. arXiv:1910.02547  
 Jewitt D., Luu J., Rajagopal J., Kotulla R., Ridgway S., Liu W., Augusteijn T., 2017, *ApJ*, **850**, L36  
 Katz J. I., 2018, *MNRAS*, **478**, L95  
 Lester T. P., McCall M. L., Tatum J. B., 1979, *J. R. Astron. Soc. Canada*, **73**, 233  
 Lumme K., Bowell E., 1981, *AJ*, **86**, 1694  
 Mashchenko S., 2019, arXiv e-prints, p. arXiv:1906.03696  
 McNeill A., Trilling D. E., Mommert M., 2018, *ApJ*, **857**, L1  
 Meech K. J., et al., 2017, *Nature*, **552**, 378  
 Muinonen K., Lumme K., 2015, *A&A*, **584**, A23  
 'Oumuamua ISSI Team 2019, *Nature Astronomy*, **3**, 594  
 Raymond S. N., Armitage P. J., Veras D., 2018, *ApJ*, **856**, L7  
 Siraj A., Loeb A., 2019, *Research Notes of the American Astronomical Society*, **3**, 15  
 Trilling D. E., et al., 2018, *AJ*, **156**, 261